

SPREADING OF THE AMAZON RIVER PLUME

Eugene G. Morozov^{*,1,5} , Peter O. Zavialov¹, Victor V. Zamshin², Osmar O. Moller Jr.³ , Dmitry I. Frey^{1,4,5} , Oleg A. Zuev¹ , Anna M. Seliverstova¹ , Alexey V. Bulanov⁶, Nadezhda A. Lipinskaya⁶, Pavel A. Salyuk⁶, Olga I. Chvertkova², Inna A. Nemirovskaya¹, Viktor A. Krechik¹ , and Anna L. Chultsova¹

¹Shirshov Institute of Oceanology, Russian Academy of Sciences, Moscow, Russia

²AEROCOSMOS Research Institute for Aerospace Monitoring, Moscow, Russia

³Federal University of the State of Rio Grande, Porto Alegre RS, Rio Grande, Brazil

⁴Marine Hydrophysical Institute, Russian Academy of Sciences, Sevastopol, Russia

⁵Moscow Institute of Physics and Technology, Dolgoprudny, Russia

⁶V. I. Il'ichev Pacific Oceanological Institute, Far Eastern Branch of RAS, Vladivostok, Russia

* **Correspondence to:** Eugene G. Morozov, egmorozov@mail.ru

Abstract: Results of a joint Russian-Brazilian expedition to study the dynamics of continental river runoff in the ocean associated with the Amazon plume are presented. The stations of the study region covered the seaward part of the Amazon plume. The work was carried out in the dry season (November). The data of in situ measurements and satellite data show that the most desalinated and rich in suspended particulate matter and chlorophyll-a waters were localized on the shallow inner shelf. The horizontal and vertical structure of the thermohaline fields indicates the presence of a well-pronounced river plume about 15 m thick. The decrease in salinity in the plume relative to the background values exceeded 6 PSU even at 300–400 km from the river mouth. The plume waters were characterized by increased concentrations of suspended matter. The best approximation to the in situ measurements is provided by the SMOS satellite salinity data and reanalysis GLORYS12. Chemical determinations in the surface layer in the area of the plume reveal elevated concentrations of silicates, phosphates, and nitrites compared to the seaward part.

Keywords: Amazon plume, satellite images, CTD casts, chlorophyll-a, frontal zone, suspended particular matter

Citation: Morozov E. G., Zavialov P. O., Zamshin V. V., Moller Jr. O. O., Frey D. I., Zuev O. A., Seliverstova A. M., Bulanov A. V., Lipinskaya N. A., Salyuk P. A., Chvertkova O. I., Nemirovskaya I. A., Krechik V. A., and Chultsova A. L. (2023), Spreading of the Amazon River Plume, *Russ. J. Earth. Sci.*, 23, ES4006, <https://doi.org/10.2205/2023es000863>

Introduction

River plumes are dynamic structures in the ocean, which are the main links of interaction between the ocean and land and the main carriers of pollution. Plumes from large river mouths can occupy hundreds of thousands of square kilometers in the ocean; they form the regime of the active layer of the ocean in vast water areas, on shelves, on continental slopes, and in open parts of the ocean affected by runoff.

Atlantic waters off the coast of South America are the most interesting region of the World Ocean in terms of studying the global role of continental runoff. The Amazon River is a unique region of the Earth with a huge catchment area. Its length is almost 7000 km. The Amazon freshwater runoff reaches 0.20 Sv (0.20 Sv = 10^6 m³/s) or 6300 km³/year, with an average value of 5500 km³/year [Nordin and Meade, 1985], (6300 km³/year is approximately 200,000 m³/s). For comparison, the average flow from the Yenisei River is only about 18,000 m³/s, and the runoff of the Volga is about 8000 m³/s.

The main source of Amazon waters is evaporation from the Atlantic, which is transported by the trade winds from the Atlantic Ocean to the west and falls as rain. A large amount of moisture is deposited on the eastern slopes of the Andes. Precipitation here reaches 3000 mm/year. The water balance of the Amazon is estimated as follows:

RESEARCH ARTICLE

Received: 24 May 2023

Accepted: 19 July 2023

Published: 26 October 2023



Copyright: © 2023. The Authors. This article is an open access article distributed under the terms and conditions of the Creative Commons Attribution (CC BY) license (<https://creativecommons.org/licenses/by/4.0/>).

- Precipitation: 12×10^{12} m³/year or 12,000 km³/year;
- Runoff into the ocean: 5500 km³/year;
- Evaporation: 6500 km³/year.

The annual mean precipitation in the rainforest regions of Amazonia is 2942 mm; the wet season is in March–June (>320 mm/month) and the minimum is in August–December (140 mm/month) [*Aventura do Brasil*, 2023; *Ecuador & Galapagos Insiders*, 2023]. The Amazon plume extends to the northwest from the river mouth under the influence of the trade winds and the North Brazil Current. The current core is located on the continental slope, and the plume is located at shallow depths on the shelf.

According to the results of recent studies [e.g., *Varona et al.*, 2019], dynamics of the Amazon plume significantly affects the regime of the entire equatorial part of the Atlantic Ocean [*Jo*, 2005; *Muller-Karger et al.*, 1988] (at least within the square 60°–24°W and 5°S–16°N), reducing surface salinity by 4–8 PSU and the thickness of the upper quasi-homogeneous layer by 15–50 m. The plume also reduces the heat content of the ocean due to the “barrier effect” even at a large distance from the mouth (up to 4000 km and further), as well as increasing the eastward transport of currents. The quantitative aspects of this influence remain poorly understood.

In March 1983, an expedition of the Shirshov Institute of Oceanology onboard the R/V *Professor Shtokman* (cruise 9) performed measurements at the mouth of the Amazon River and upstream the river reaching the city of Manaus and further upstream along the Rio Negro River [*Monin and Gordeev*, 1988]. Almost 40 years later, we again turned to the study of the Amazon River outflow in the context of current scientific problems, as well as in the new conditions of the Earth’s climate system. We are interested in the influence of the Amazon on many processes in the ocean. In November 2022, an expedition onboard the Russian R/V *Akademik Boris Petrov* (cruise 52) worked in the region of the Amazon plume together with the leading oceanographers from Brazil.

Since the previous joint work in 1983 we entered the era of satellite oceanography. The goal of our expedition and this publication was to analyze the new data of field measurements and interpret them together with the available satellite observations of the region to get a new comprehensive view on the processes in this important region of the ocean.

Data and Methods

This study is based on the oceanographic and optical data combined with the satellite observations. The measurements over the survey region at 28 stations were carried out using a CTD probe up to 200 m and water sampling with Niskin bottles close to the surface. An AML Oceanographic BaseX CTD probe was used for these measurements. Sampling rate was set to 20 Hz, the CTD vertical speed was 1 m/s, which gives the initial vertical resolution equal to 0.25 m. Only downcast data were used as the CTD profile data. The standard SeaCast software (Version 4.4.0) was used for the data collection. The LADCP data measured by TRDI WorkHorse Monitor 300 kHz profiler were processed using programming package LDEO Software version IX.10 [*Visbeck*, 2002].

Temperature and salinity were continuously measured using the SeaBird SBE-45 flow-through thermosalinograph, into which water was supplied approximately from a depth of 5 m during the motion of the ship with a time step of 10 s. The resulting values have been corrected using the AML Oceanographic BaseX CTD data to eliminate the effect of the flow-through system.

Studies of suspended particulate matter included its separation under a vacuum of 400 mbar on polycarbonate nuclear filters (pore size 0.45 μm, cloth produced at the Joint Institute of Nuclear Research in Dubna), which were preliminarily washed with hydrochloric acid. To obtain reliable results, the determination was carried out on three parallel filters, which were weighed in a stationary laboratory with an accuracy of 0.000,01 g. The composition of the suspended particulate matter was studied using a VEGA-3sem scanning electron microscope, TESCAN (Czech Republic).

The contents of the main forms of nutrients were determined: inorganic forms of silicates, mineral phosphorus, nitrate, nitrite, dissolved oxygen, total alkalinity, and pH. Further processing of samples for the study of all these parameters was carried out in the onboard laboratory immediately after sampling. Water samples were taken with Niskin bottles from the surface and processed after 6–12 hours using standard methods adopted in marine chemistry [Bordovsky and Chernyakova, 1992]. All samples were preliminarily filtered through nuclear filters with a pore diameter of 0.45 μm .

Bio-optical measurements were carried out using a Turner C6P profiling hydrooptical probe, which measures the intensity of chlorophyll-a (chl-a) and colored dissolved organic matter (CDOM) fluorescence, as well as turbidity, to the depths not exceeding 300 m with a frequency of 1 Hz. The chl-a fluorescence intensities were converted into chl-a mass concentrations ($C_{\text{chl-a}}$, mg/m^3) by comparison with the standard extract spectrophotometric method [Jeffrey and Humphrey, 1975]. The CDOM fluorescence intensity was calibrated to the Quinine Sulfate units (QSU) and turbidity values to formazin turbidity units (FTU) under laboratory conditions just before the expedition.

Field studies in the study site in the zone of mixing of the river and sea waters on the Amazon shelf were conducted from November 22 to 28, 2022. Locations of stations during our survey superimposed on the bathymetry chart are shown in Figure 1. During our survey in the Amazon delta region, 28 stations were made over sections located normal to the coastline, from 2 to 6 stations over each section. LADCP current measurements were made only at a few stations. When planning work, we used the current satellite information provided by the AEROCOSMOS Research Institute. Collection, processing, systematization, and storage of heterogeneous space data were carried out using a special information infrastructure previously developed at the AEROCOSMOS Research Institute. Preliminary information products of satellite oceanography were sent to the ship. In the period from October 15 to November 25, 2022, four updates of the spatial distributions were sent to the ship.

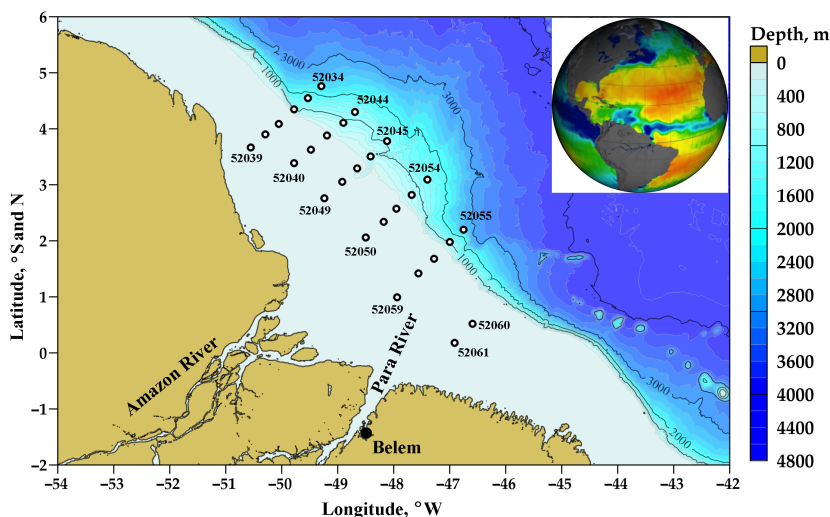


Figure 1. Topography of the study region based on the GEMCO 2022 data and points of our stations with numbers. The inset shows surface salinity in the Atlantic demonstrating the global influence of the Amazon River on Atlantic salinity as depicted on the NOAA website (https://salinity.oceansciences.org/quiz_salty_fresh.htm).

The satellite information products used in the planning of ship operations and in the analysis, which are presented in this article, include:

- chl-a concentrations based on the GCOM-C data [Murakami, 2020],
- particulate organic carbon concentrations based on the TERRA MODIS data [NASA Ocean Biology Processing Group, 2018],

- sea surface temperatures (satellite products based on the AQUA, TERRA MODIS data [NASA Ocean Biology Processing Group, 2020a,b], satellite products based on the GCOM-C data [Kurihara, 2020], model products based on the NOAA OISST data [Reynolds et al., 2008],
- salinity of the sea surface and water column (satellite products based on the SMAP data [Fore et al., 2016], satellite products based on the SMOS data [Barcelona Expert Center, 2016]),
- spectral characteristics of the sea surface in natural colors (Sentinel-3A/B multispectral space images [Donlon et al., 2012], SeaHawk CubeSat multispectral space images [NASA Ocean Biology Processing Group, 2021]).

Regional Settings

We used previously published information when planning work. According to satellite data and many other observations, the Amazon plume propagates to the northwest in the shallow coastal part of the shelf. The seasonal variability of temperature and salinity in the Amazon plume was considered in [Smith and Demaster, 1996] based on the data of four expeditions onboard the R/V *Columbus Iselin* in 1989–1991. The surveys were carried out according to the scheme, which was similar to our scheme of stations, but they were able to work at shallower depths. Salinity distribution based on four surveys of this experiment is shown in Figure 2.

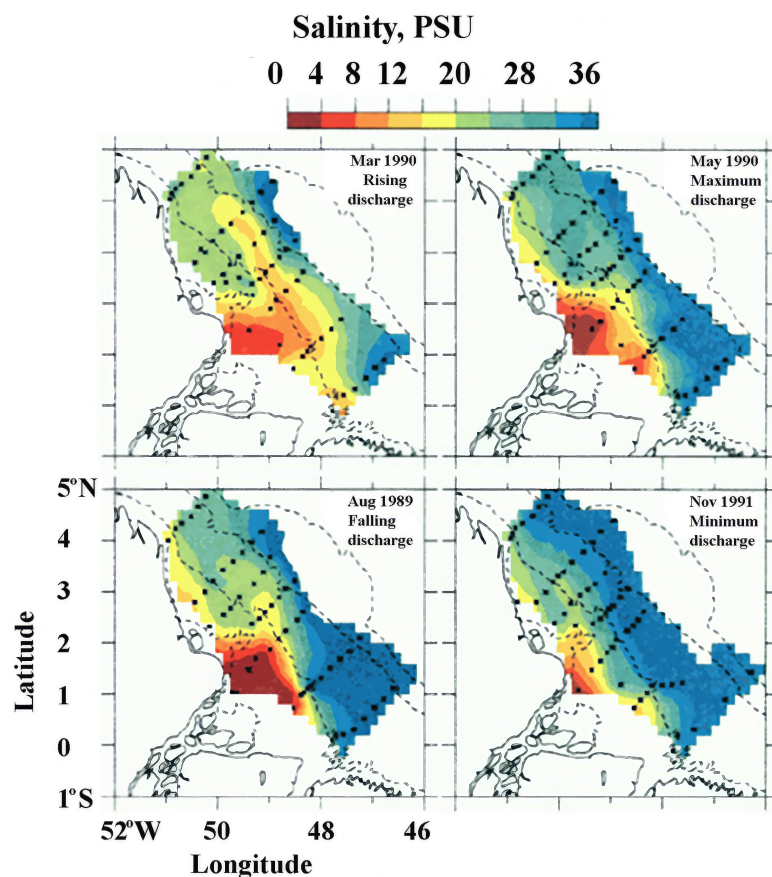


Figure 2. Maps of surface salinity (color scale) based on four surveys in 1989–1991 [Lentz and Limeburner, 1995]. Black dots indicate CTD stations. The dashed lines are the 5, 20, 100, and 1000-m isobaths.

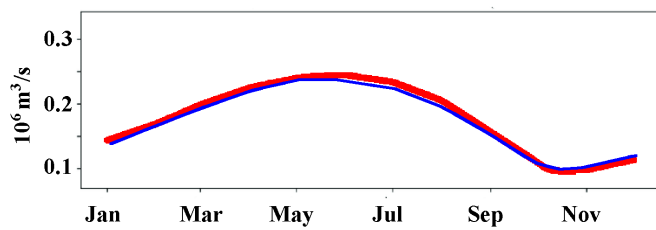


Figure 3. Seasonal runoff cycle of the Amazon. Data from measurements at Óbidos stream gauge station 700 km from the ocean (red line [Giffard *et al.*, 2019]; blue line [Dai and Trenberth, 2002; Liang *et al.*, 2020]).

The authors of [Smith and Demaster, 1996] distinguish three zones: the coastal zone of turbid waters with suspended particular matter concentration exceeding 10 mg/L; plume boundary zone with concentration less than 10 mg/L and salinity less than 32 PSU; and an offshore zone with a salinity greater than 32 PSU. The highest chl-a concentrations were measured in the narrow intermediate zone of the plume boundary outside the turbid low-salinity waters. Intermediate values were found in low-salinity turbid waters near the coast and river mouth, and low concentrations were in high-salinity waters away from the coast. The maximum surface chl-a levels for peak and minimum discharge periods were 25.5 and 3.8 mL/L, respectively.

The concentration of nutrients was maximum in the coastal zone up to 7 μM , in the intermediate zone the concentration was about 0.5 μM , and in the seaward zone, they were even lower. The maxima of chl-a and nutrients were observed in the subsurface layer at a depth of about 5 m.

In addition, SMAP ocean surface salinity satellite data in 2019 were analyzed. Satellite images show strong variability in the Amazon runoff and plume propagation. Plume development begins in April and reaches a maximum in July–August, in contrast to the seasonality of rains, which are maximum in March. After maximum precipitation (which is over the rainforests far from the coast), water should drain into the river from the catchment area, flow downstream, and only after this the maximum discharge of fresh water into the ocean occurs. The flow of water in the Amazon was measured near the city of Óbidos, which is 700 km from the river mouth. The maximum was observed here in May–June (Figure 3).

Figure 4 shows annual variability of the Amazon plume based on satellite salinity data in 2019. Similar variability is discussed in [Hu *et al.*, 2004] based on direct measurements and satellite images. The authors provide monthly maps of the Amazon plume in 1988–1991.

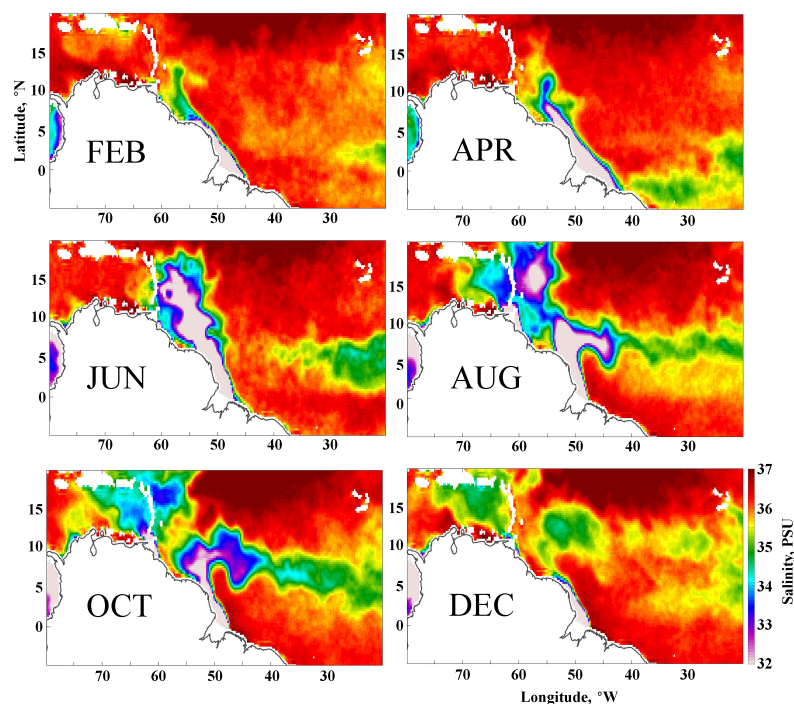


Figure 4. Annual salinity variations in the Amazon plume based on SMAP satellite data in 2019.

Salinity map near the Amazon mouth is shown in Figure 5 based on the measurements in 1983, during the cruise of the R/V *Professor Shtokman* [Monin and Gordeev, 1988]. The grid of our stations in 2022 is superimposed on this map. The most important difference in measurements is related to seasonality. The cruise of the R/V *Professor Shtokman* was in March 1983 during the period of high runoff of the Amazon in contrast to our measurements in November 2022 during the driest period. In different seasons, the runoff of the Amazon differs several times, and similarly, the Amazon plume narrows and expands. The 35 PSU isotherm displaced by about 30 miles closer to the coast compared to its location in March 1983.

Salinity isoline 35 PSU is shown in Figure 5 based on the GLORIS12 reanalysis data for November 2022. Salinity 30 PSU based on our in situ measurements was found only at the southwestern point of the station grid.

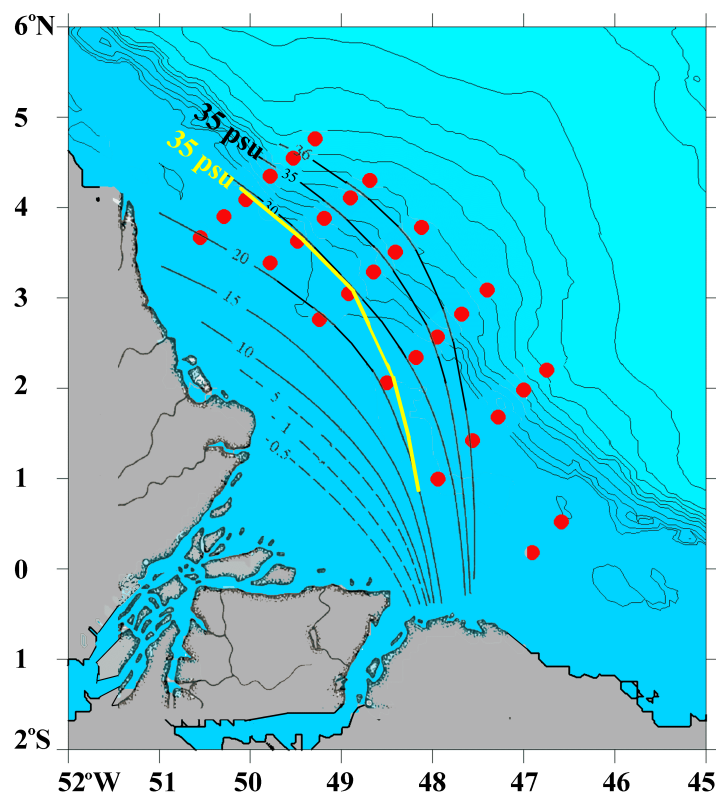


Figure 5. Map of salinity isolines (PSU) based on the data of the R/V *Professor Shtokman* cruise in 1983 (black isolines) [Monin and Gordeev, 1988]. Our 2022 station points are shown in red. The yellow line shows the surface salinity contour of 35 PSU according to the GLORYS12 reanalysis data for November 2022.

The most recent research in remote sensing of the Amazon plume is given in [Yu *et al.*, 2022]. The authors studied suspended particulate matter in the delta and plume. They revealed that the Amazon estuary has a “filter effect”. Concentration of suspended particulate matter was high in the nearshore area and lower offshore. Most of the suspended particulate matter accumulated within the estuary in a fan shape. Research presented in [Geyer *et al.*, 1996] suggests that suspended particulate matter in the shallow regions of the Amazon estuary and shelf region northwest of the river is higher than that in the Amazon River, which can be caused by resuspension and strong mixing due to tides. Curtin and Legeckis [1986] report that during peak discharge concentrations of suspended particulate matter exceeding 0.01 g/L at the surface extend over a distance of 200 m in the Amazon plume.

Data Analysis and Discussion

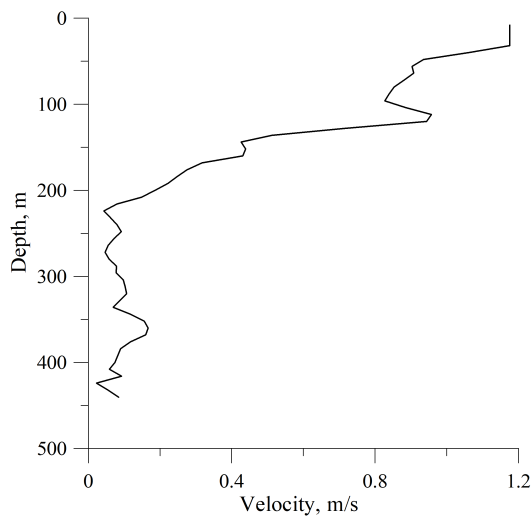


Figure 6. Profile of the current velocity at station 52046 ($3^{\circ}30.74'N$, $48^{\circ}24.66'W$) on the continental slope on November 11, 2022. The direction of the vector is northwest 315° .

The velocities that we measured with LADCP at a few stations were high: more than two knots (100 cm/s) to the northwest. At a depth of 200 m, the current velocities decrease to lower than 20 cm/s (Figure 6). The ocean in this part of the shelf is shallower than 20 m, where the vessel could not enter. The curve of the northern coastline here forces the fresh water from the Amazon River to run closer to the coast and be reinforced by the outflow [Magliocca, 1971]. Judging by the spatial distribution of salinity recorded during field works, the stations of the study area were mostly in the offshore part of the Amazon River plume and its periphery above the continental slope, as well as the outer water area of ocean waters.

The satellite data over the period of the field works show that the most desalinated and rich in suspended particulate matter and chl-a waters were localized on the inner shelf. At the same time, in the area covered by ship measurements, salinity did not decrease below 30 PSU. Nevertheless, the horizontal and vertical structure of the thermo-haline fields indicates the presence of a well-defined river plume (Figure 7) about 15 m thick, which forms a vertical stratification. The decrease in salinity in the plume relative to the background values was more than 6 PSU even at 300–400 km from the mouth. Water desalination due to the flow of fresh water from the Amazon in the area of the plume extends to the depths of about 10–15 m. Salinity section normal to the coast (Figure 8) clearly shows the region of the

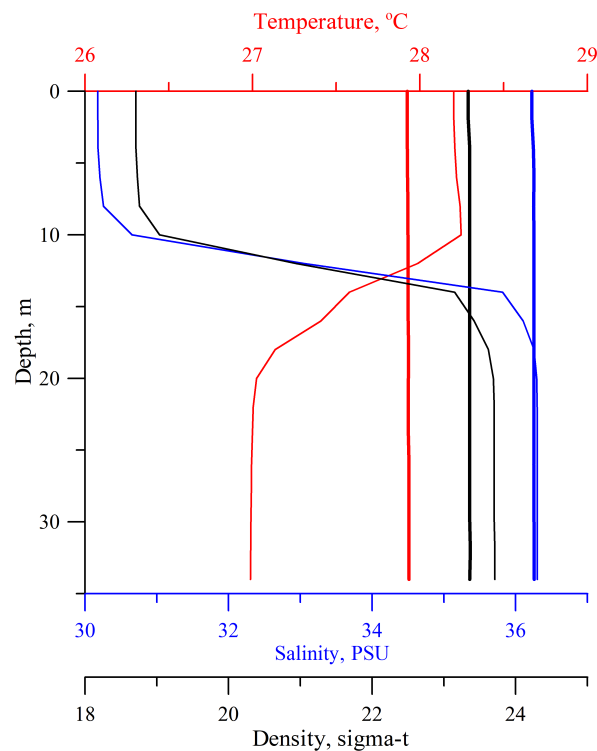


Figure 7. Vertical profiles of salinity (blue curves), temperature (red curves), and density (black curves) in the upper layer of the ocean within the Amazon plume (thin lines, station 52039) and outside it (thick lines, station 52034).

plume, decreased salinity in the upper layer caused by long-term spreading of the plume and wind mixing, and salinity maximum below low salinities in the upper layer.

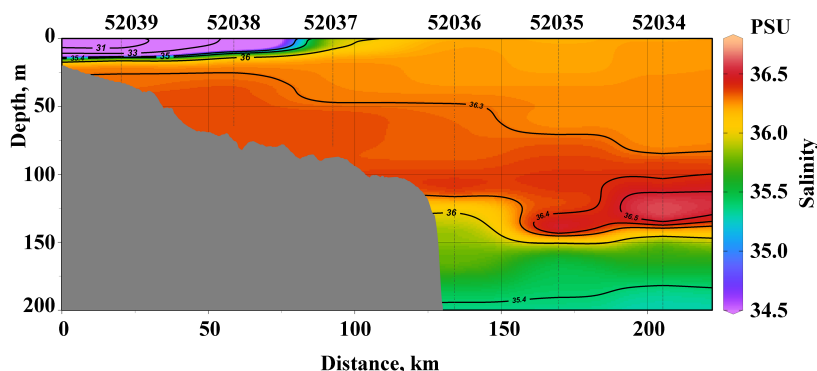


Figure 8. Salinity section from station 52034 to station 52039.

Figure 9 shows several salinity contour lines on the ocean surface based on our survey with the AML-probe and two reanalyses. The AML survey almost coincides with the data from the SBE19 instrument in the ship's flow-through system. The best approximation to the field data is provided by satellite data on salinity SMOS and reanalysis GLORYS12.

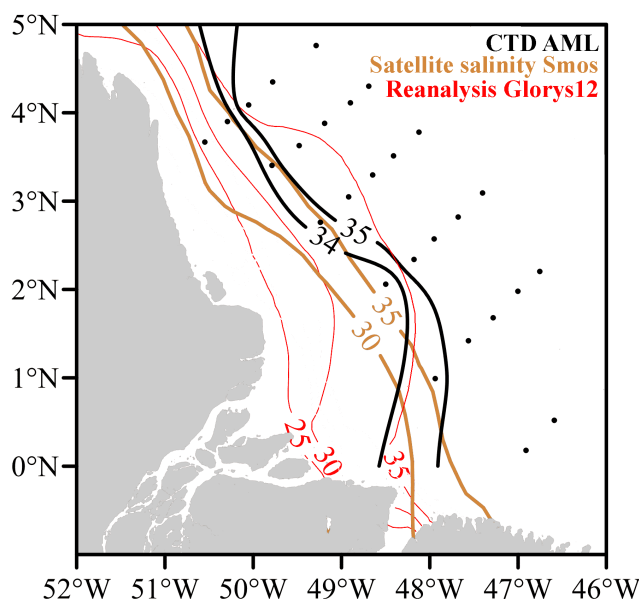


Figure 9. Surface salinity from the GLORYS12 reanalyses, surface salinity satellite data (SMOS), and survey results (AML data).

The flow-through system of the ship installed to let the surface water flow made it possible to map the surface salinity also in the Para River (a branch in the Amazon delta). At the entrance to the river, salinity sharply decreases to the values in the freshwater bay. The measurements stopped at a salinity of 30 PSU (**Figure 10**).

Let us compare our measurements in the region with the data of historical CTD casts. Surface salinity based on the data of our survey using the flow-through system is shown in **Figure 10a**. The position of the plume according to the GLORYS12 reanalysis data in November 2022 is shown in **Figure 10b**. The GLORYS12 reanalysis data show similar distribution of salinity at the surface. It provides data in the regions inaccessible for the ship measurement. One can see that our survey covers only the outer boundary of the plume and almost does not cover the region of the plume itself, since it is located at shallow depths. Sea surface temperature based on the GLORYS12 data is higher near the coast

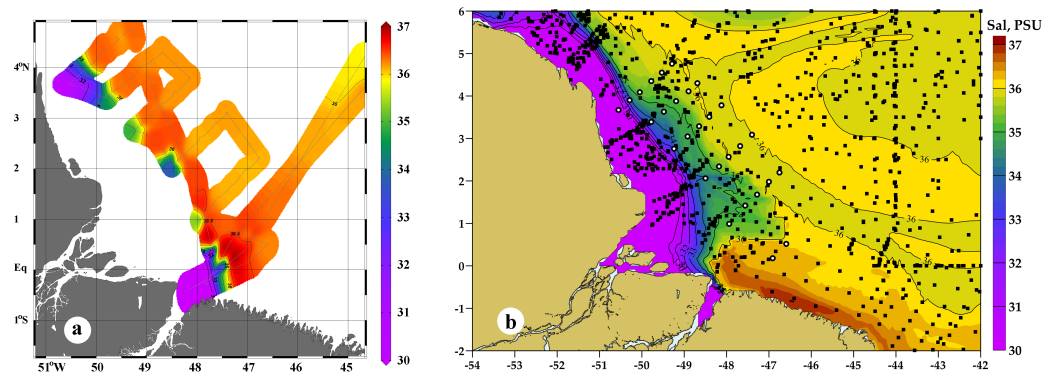


Figure 10. Surface salinity map based on the data of the flow-through system and map of the ship route (thin lines) (a). Historical CTD-measurements in the region based on the WOD18 database (black dots) [Boyer et al., 2018]. The background surface salinity is shown based on the GLORYS12 reanalysis for November 21, 2022 [Lellouche et al., 2021]. Our stations are shown with white circles (b).

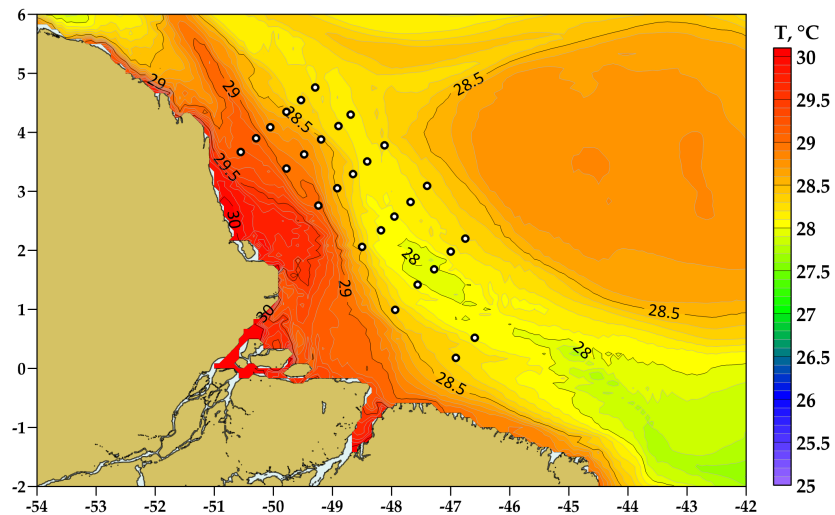


Figure 11. Sea surface temperature map based on the GLORYS12 reanalysis data on November 21, 2022. Our stations are shown with white circles.

in the Amazon plume and decreases in the outer shelf region (Figure 10b). Sea surface temperature based on the GLORYS12 reanalysis is shown in Figure 11.

The distribution of total titratable alkalinity and dissolved silicates correlates well with the distribution of temperature and salinity (Figure 12). These parameters can be also used as markers of the river runoff. The lowest values of total alkalinity (2038–2200 μM) and the highest values of dissolved silicates (8.95–12.32 μM) were observed at coastal stations 52039 and 52050. Total alkalinity increased and silicates decreased to 2433 μM (stations 52048 and 52031) and 0.45–0.55 μM (stations 52036 and 52032), respectively with the distance from the coast and from the river plume.

The pH values varied from 8.18 to 8.23 (average is 8.19). The minimum values were recorded at stations 52049 and 52040. The maximum values were recorded at station 52038, since the Amazon waters are characterized by low pH values (4–5 units of the pH scale).

The concentration of dissolved oxygen in the study region ranged from 4.35 to 4.95 mL/L (94–111% saturation) (Figure 13). The maxima were recorded at stations 52038 and 52040 (4.94–4.95 mL/L, at 110–111% saturation), minima, at stations 52049 and 52039 (4.35 mL/L, at 94–98% saturation). Such low concentrations of dissolved oxygen are characteristic of this region [Lyakhin, 1990]; however, a high percentage of water saturation with oxygen indicates active photosynthesis processes.

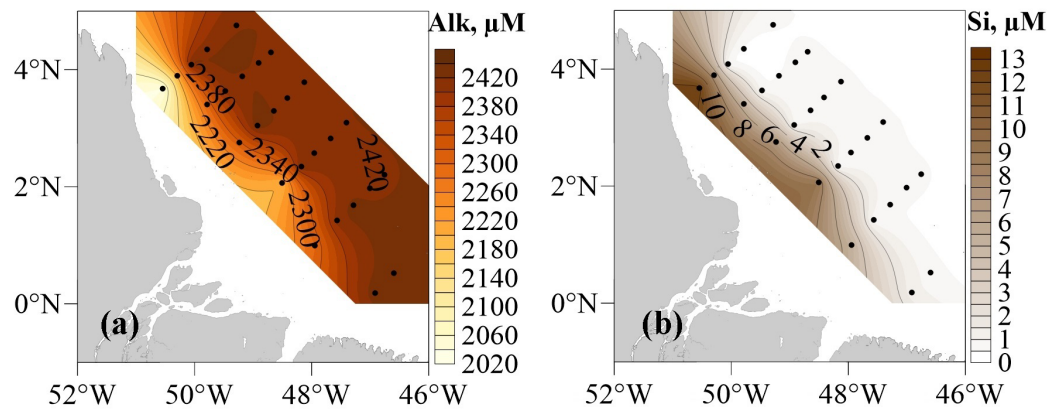


Figure 12. Maps of the surface distribution of alkalinity (a) and silicates (b). Our stations are indicated with black dots.

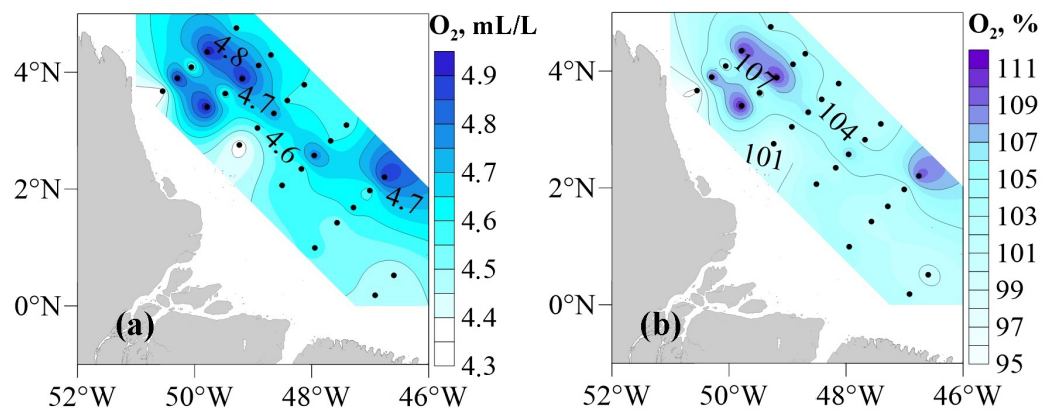


Figure 13. Maps of the surface distribution of dissolved oxygen (a) and oxygen saturation (b) at the surface. Our stations are indicated with black dots.

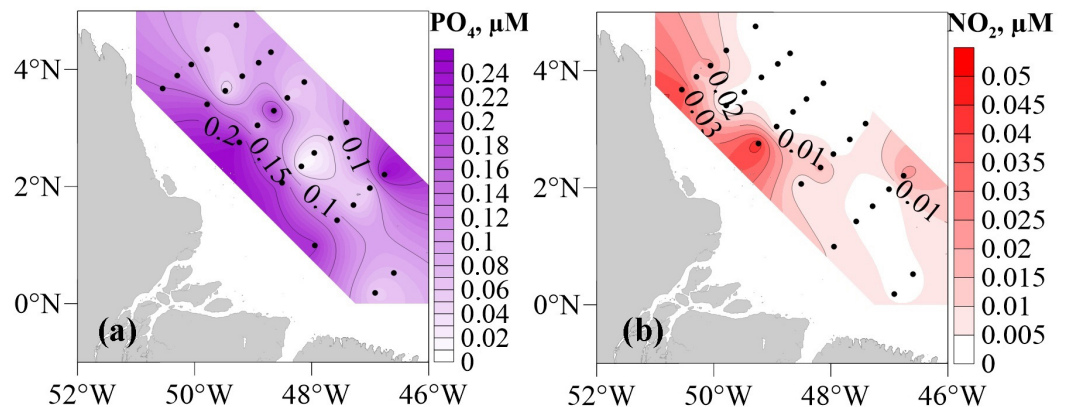


Figure 14. Maps of the surface distribution of phosphorus (a) and nitrites (b).

The content of dissolved phosphorus, nitrates, and nitrites in the study region was extremely low, averaging 0.10, 0.14, and 0 μM , respectively. Local maxima of their content were located near the coastal stations in the region of the plume. The distribution of nitrates was more uniform over the study area. At station 52049, the amount of dissolved phosphorus was 0.23 μM , nitrates, 0.20 μM , and nitrites, 0.04 μM ; in the offshore region they decreased almost to zero (Figure 14). This conclusion correlates with the results in [Smith and Demaster, 1996].

We note that at station 52040 maxima of dissolved oxygen and local minima of nitrates and nitrites were observed, and at station 52049 we recorded maxima of phosphates, nitrates and nitrites, and minimum of dissolved oxygen.

Spatial distributions of nutrient concentrations in the plume of the Amazon River were studied based on interpolated satellite data on the concentration of chl-a (mg/m^3), formed for each day of the expedition period (from November 22 to November 28, inclusive) based on the combined data from the S-NPP VIIRS, NOAA-20 VIIRS, and Sentinel-3A OLCI satellite radiometers [Wang *et al.*, 2017]. An image for November 28 is shown in Figure 15. To identify the conditional boundaries of the plume of the Amazon River and calculating its area, a threshold value of $\geq 3 \text{ mg}/\text{m}^3$ was applied to each spatial distribution of chl-a concentration. The square of the region with high concentration S ($\geq 3 \text{ mg}/\text{m}^3$) was calculated from the number of pixels in the image. Within the week of observations it varied from 91,530 to 99,468 km^2 .

One should keep in mind that satellite estimates of chl-a concentrations in the Amazon plume include a large portion of CDOM [Del Vecchio, 2004]. The authors emphasize that comparisons of satellite-derived chl-a concentrations with in situ High-performance liquid chromatography (HPLC) based measurements showed an overestimation due to additional CDOM light absorption. Therefore, the satellite data on the concentration of chl-a in the study area should be interpreted as a sum of the concentration of chl-a and the content of CDOM.

According to satellite maps of the distribution of chl-a in the study region, its maximum was generally in the Amazon plume. Beyond the plume, the chl-a concentration sharply decreased. Generally, emission of chl-a to the ocean was recorded from the main river stream of the Amazon, not from the branch of the delta (Para River), in which Belem is located.

The plume of the Amazon River identified by the threshold cutoff of chl-a concentration $\geq 3 \text{ mg}/\text{m}^3$ in the period from November 22 to 28, 2022, was characterized by an almost unchanged contour and a slightly changing area, the values of which varied from 91,530 to 99,468 km^2 . It was found that the chl-a concentration reached significantly high values ($15 \text{ mg}/\text{m}^3$) in the tip of the eastern bay (Para River) at about 100 km from the coastline into the continent. Since the runoff of freshwater from the Para River is low, these chl-a is not transported into the ocean.

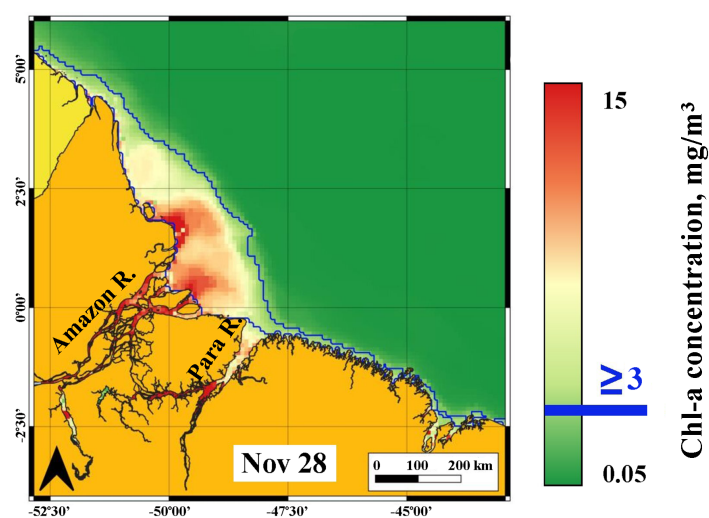


Figure 15. Spatial distributions of chl-a concentration (mg/m^3) on the surface based on the satellite radiometers SNPP VIIRS, NOAA-20 VIIRS, and Sentinel-3A OLCI on November 28, 2022 using the algorithm in [Wang *et al.*, 2017]. Blue isoline shows the boundary of concentration $3 \text{ mg}/\text{m}^3$.

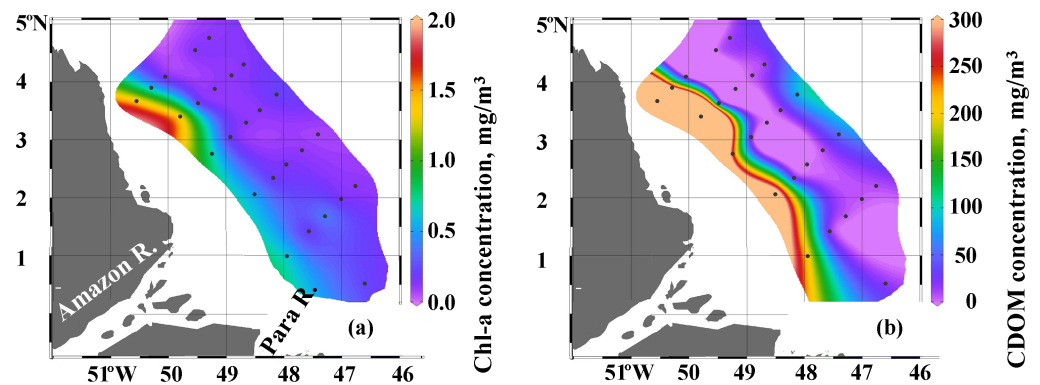


Figure 16. Map of chl-a concentration at the surface based on in situ data from stations (mg/m^3) measured using the Turner C6P instrument (a); Map of concentration of dissolved organic matter (CDOM, QSU in mg/m^3) based on the in situ data at stations measured using the Turner C6P instrument (b).

The spatial distribution of chl-a concentration was also measured at stations using the Turner C6P instrument (Figure 16). The spatial distribution of chl-a also corresponds to the results in [Smith and Demaster, 1996]. The maximum was observed at the boundary of the plume and the concentration decreased in the open ocean. The maximum of chl-a spread from the main river stream of the Amazon.

The depth distribution of chl-a as a function of the distance along the section normal to the coast is shown in Figure 17. The maximum was found in the upper ocean layer of the plume, the second maximum was at the depths of 50–70 m, which corresponds to the results of [Smith and Demaster, 1996].

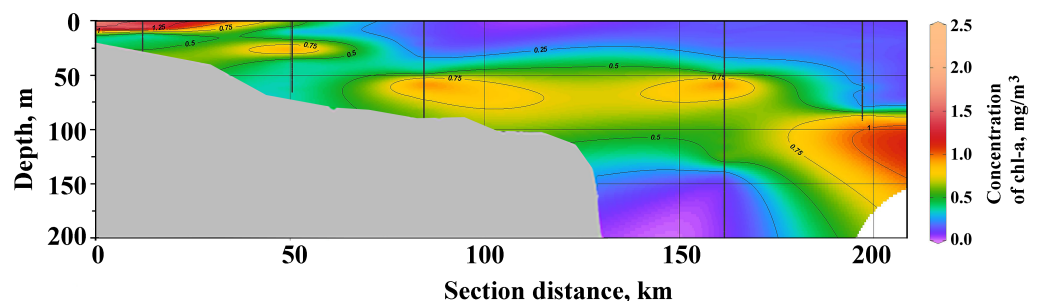


Figure 17. Concentration of chl-a (mg/m^3) along the section between stations 52034 and 52039 measured using the Turner C6P instrument. Bold vertical lines indicate stations.

Spatial distribution of the concentration of CDOM based on in situ data (Figure 16b) is similar to the distribution of satellite-derived particulate organic carbon (POC) in the discharge region of the river (Figure 18). The maximum values are determined by the flow of the river waters.

It was found that the satellite estimations of the particulate organic carbon concentrations in the processed part of the plume and in the right branch of the river delta (Para River) in the area of the Belem city reached relatively high values together with the distribution of satellite chl-a.

In addition to the spatial distributions of the satellite-derived chl-a concentration, similar distributions of the concentration of particulate organic carbon formed on each day of the expedition period (from November 22 to 28, inclusive) were studied based on the Aqua, Terra MODIS data [NASA Ocean Biology Processing Group, 2018, 2022]. Unlike the data on the interpolated products on the concentration of chl-a, the spatial distributions of the concentration of POC have a non-continuous coverage of the study site. The daily

distributions were averaged over the entire period of the expedition from November 22 to 28, 2022 to form a denser coverage (Figure 18).

The standard POC algorithm was developed for the global open ocean with POC concentrations ranging between 10 and 270 mg/m³ [Stramski et al., 2008] and was applied by NASA to routinely generate POC products. But it usually results in overestimation of POC concentration in coastal waters with complex optical properties and multiple POC sources [Chen et al., 2022; Son and Wang, 2012] due to additional CDOM influence [Le et al., 2018]. Therefore, some regional algorithms have been developed for different regions [Le et al., 2017; Liu et al., 2015]. In our work we used standard POC data to analyze the spatial distribution of the parameter.

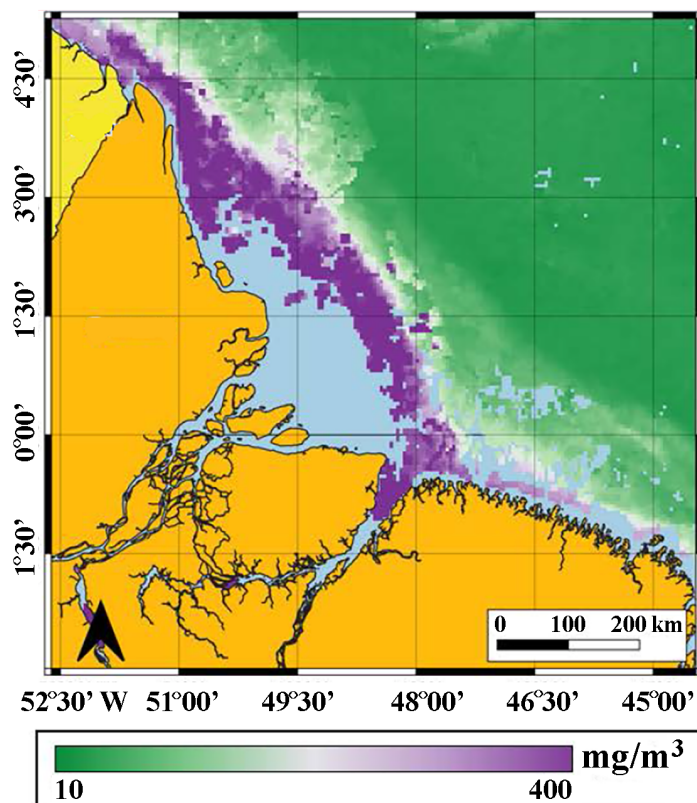


Figure 18. Mean spatial distribution of POC concentration based on the Aqua, Terra MODIS data from November 22 to 28, 2022 from the datasets [NASA Ocean Biology Processing Group, 2018, 2022] Blue color indicates lack of data.

Analysis of Figure 18 indicates that the boundaries of the Amazon River plume are not less clearly traced by the MODIS-derived distribution of concentration of POC, whose values along the plume perimeter change sharply from ≤ 20 mg/m³ to ≥ 400 mg/m³. Also, the concentrations of suspended organic matter immediately in the main river channel were not determined.

Spatial distributions of concentrations of suspended particulate matter in the area of the alluvial fan of the Amazon River were studied based on the corresponding interpolated satellite data generated for each day of the expedition period (from November 22 to 28, 2023, inclusive) based on the combined data from the S-NPP VIIRS, NOAA-20 VIIRS, and Sentinel-3A OLCI satellite radiometers [Wang et al., 2017] (Figure 19a). The highest concentrations were found at the mouth of the main channel of the Amazon River and continued along the coast north of the main channel. Lower concentrations were found in the bay, in which the port of Belem is located (Para River).

It was found that the studied concentrations in the period from November 22 to 28, 2022, as well as the previously studied concentrations of chl-a, were characterized by the

spatial distribution in the study site that remained almost unchanged over the observation period, allowing one to clearly track the plume of the Amazon River in the open ocean at the stations.

In addition, suspended particulate matter has been measured in the water samples from the surface at stations. A map of the concentration of suspended particulate matter at the surface is shown in Figure 19b based on in situ data. This map also shows that the peak concentration was found near the region of the continuation of the flow from the main branch of the river. In surface waters (Figure 19b), the concentrations of suspended particulate matter varied from 0.01 (station 52042) to 2.00 mg/L station 52049, closest to the Amazon River delta). The suspended particulate matter contained biogenic particles (mainly diatoms), which dominated at station 52043 (Figure 20a) on the outer shelf and at the southernmost station 52060 almost not affected by the river runoff (Figure 20c). Almost no mineral suspended particles were found here unlike the filter at station 52049, which was saturated with mineral particles and their fragments (Figure 20b). According to the optical parameters of the Secchi disk, its visibility varied from 3 m at the plume boundary to 22 m in the offshore part of the survey.

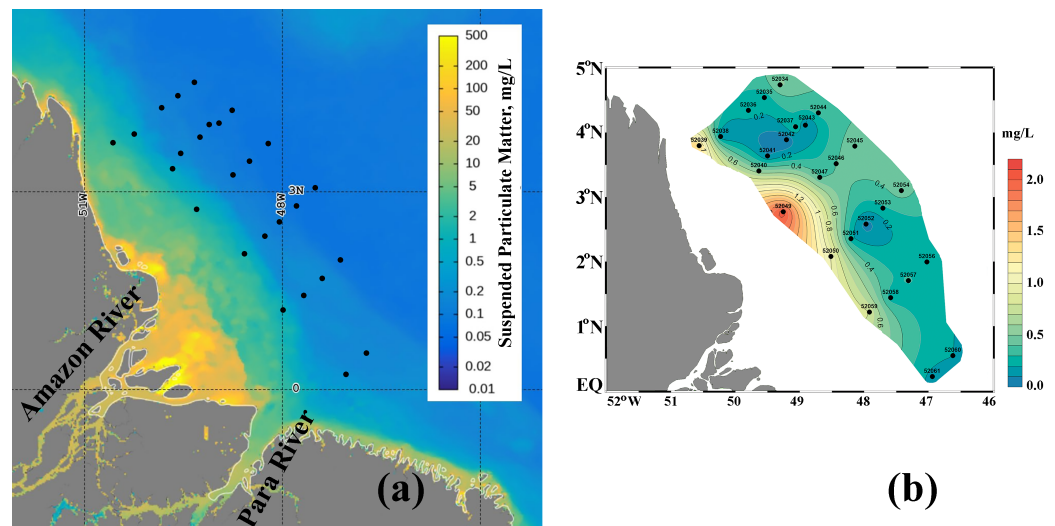


Figure 19. Spatial distributions of the concentration of suspended particulate matter at the sea surface on November 22, 2022 based on the SNPP VIIRS, NOAA-20 VIIRS, and Sentinel-3A OLCI data using the algorithm described in [Wang et al., 2017] (a). Concentration of suspended particulate matter based on the water samples from the surface at stations (b).

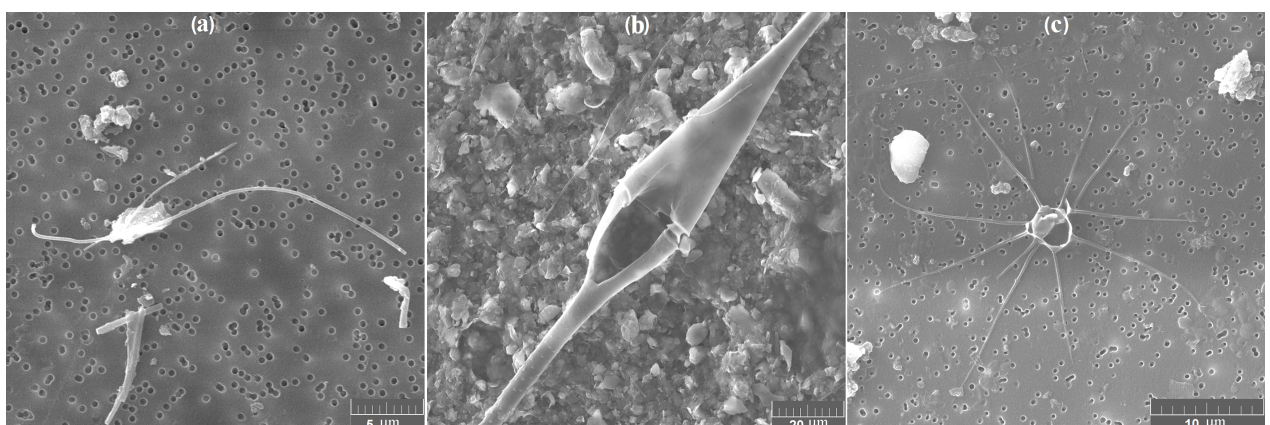


Figure 20. Suspended particulate matter composition at stations 52043 (a), 52049 (b), and 52060 (c). Mineral particles were found in the filters from station 52049.

Figure 21 shows additional data demonstrating the boundaries of the studied plume. This is a multispectral image of the sea surface from the Sentinel-3B satellite on November 23, 2022 [Donlon et al., 2012].

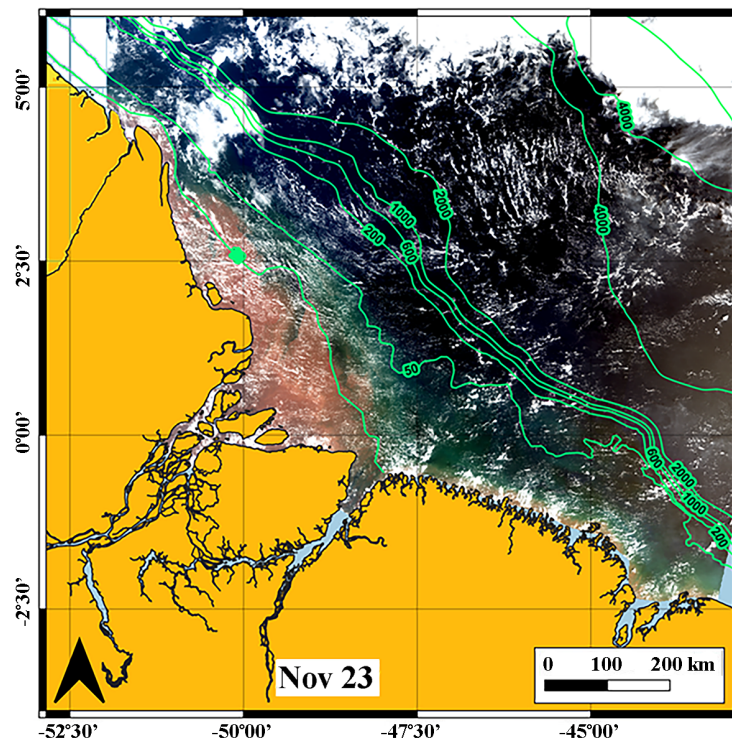


Figure 21. Multispectral satellite image of the surface in natural colors on November 23, 2022 based on the data of Sentinel-3B satellite. Isobaths of the regional bottom topography are shown.

The satellite image of the surface in natural colors (Sentinel-3B satellite) in Figure 20 gives a more detailed assessment of the plume configuration than the previous information products (presented in Figures 15, 18, 19), due to its higher spatial resolution. The image combined with the bathymetric information makes it possible to track the variability of the plume of the Amazon River in comparison with the depths of the shelf zone. It was found that the spectral characteristics of the plume surface generally follow the contours of the isobaths, which may be due to the absence of river runoff mixing with the ocean waters over shallow depths.

We emphasize that at very shallow depths, the radiation reflected from the bottom can take part in the formation of an optical image of the sea surface [Bondur, 2004; Bondur et al., 2018]. As the depth increases, the spectral characteristics of the plume of the Amazon River change. In the region of the main part of the plume (at depths up to 10 m), the waters are characterized by a saturated yellow tint, indicating high concentrations of suspended particulate matter and dissolved substances. In the area of depths in the range from 10 to 50 m, the waters acquire a less saturated shade. At depths exceeding 50 m, the plume is almost not identified by the satellite multispectral image, as a result of which the waters in this zone are characterized by a blue-green hue typical of open ocean areas. This is confirmed by visual observations and measurements with a Secchi disk.

In general, the revealed spatial distributions of suspended and dissolved organic substances in the study area are similar, but there are some peculiarities that require additional discussion. Suspended particulate matter concentration near the city of Belem based on the satellite estimates, is lower than in the area of influence of the Amazon River (Figure 20). However, according to the spatial distribution of satellite estimates of chl-a and POC concentrations, which are also largely determined by the content of CDOM (Figures 16, 18), the amount of dissolved organic matter near Belem is also large, as in the zone of influence of the Amazon River. This is also confirmed by ship data. It can be assumed that

an additional source of CDOM (but not suspended particulate matter) in the Belem region is associated with some kind of anthropogenic activity, for example, with the release of wastewater. This fact favors the idea of the greater emission of CDOM from the Belem city compared to the main stream from the river where there are no large cities.

Summary

Horizontal and vertical structure of the thermohaline fields during the dry season in the study site of the Amazon plume indicates the presence of a well-pronounced river plume about 15 m thick. The flow is driven to the northwest along the coast by wind and the North Brazil Current. Salinity in the offshore part on the shelf covered by the ship's measurements did not drop below 30 PSU. The decrease in salinity in the plume relative to the background values was more than 5 PSU even at 300–400 km from the mouth. The best approximation to the measurement data is provided by satellite data on salinity SMOS and reanalysis GLORYS12.

The data of in situ measurements and satellite data show that the most desalinated and rich in suspended particulate matter and chl-a waters were localized on the inner shelf. Waters with a high content of chl-a are carried out from the main channel of the Amazon River, which may indicate their predominantly natural origin. A stream of waters with a high concentration of colored dissolved organic matter and particulate organic carbon is carried out in the most eastern branch of the delta (Para River), where the two-million city and port of Belem is located.

Chemical determinations in the surface layer of the ocean in the plume reveal elevated values of silicates, phosphates, and nitrites compared to the seaward part.

The plume does not strongly change within a week, and ship measurements distributed over time give a relevant pattern of the plume.

Acknowledgments. The study was carried out within the framework of State Assignments FMWE-2021-0002 (ship measurements), 0211-2021-0007 (bio-optical investigations) and supported by the Russian Science Foundation grant 21-77-20004 (field data analysis and interpretation). The data of measurements can be sent on request.

References

- Aventura do Brasil (2023), Climate and Best Time to Visit the Amazon, Brazil, <https://www.aventuradobrasil.com/info/brazil-climate/amazon/>.
- Barcelona Expert Center (2016), SMOS-BEC Ocean and Land Products Description. BEC-SMOS-0001-PD, Version 1.5., *Technical report*.
- Bondur, V. G. (2004), Aerospace methods in modern oceanology, in *New Ideas in Oceanology. Vol. 1. Physics. Chemistry. Biology*, pp. 55–117, Nauka, Moscow (in Russian).
- Bondur, V. G., V. A. Ivanov, V. A. Dulov, Y. N. Goryachkin, V. V. Zamshin, S. I. Kondratiev, M. E. Lee, V. S. Mukhanov, E. E. Sovga, and A. M. Chukharev (2018), Structure and origin of the underwater plume near Sevastopol, *Fundamental and Applied Hydrophysics*, 11(4), 42–54, <https://doi.org/10.7868/S2073667318040068> (in Russian).
- Bordovsky, O. K., and A. M. Chernyakova (1992), *Modern methods of hydrochemical research of the ocean*, 201 pp., IO RAN, Moscow.
- Boyer, T. P., O. K. Baranova, C. Coleman, H. E. Garcia, A. Grodsky, R. A. Locarnini, A. V. Mishonov, C. R. Paver, J. R. Reagan, D. Seidov, I. V. Smolyar, K. W. Weathers, and M. M. Zweng (2018), *World Ocean Database 2018*, NOAA Atlas NESDIS 87.
- Chen, D., L. Zeng, K. Boot, and Q. Liu (2022), Satellite Observed Spatial and Temporal Variabilities of Particulate Organic Carbon in the East China Sea, *Remote Sensing*, 14(8), 1799, <https://doi.org/10.3390/rs14081799>.
- Curtin, T. B., and R. V. Legeckis (1986), Physical observations in the plume region of the Amazon River during peak discharge-I. Surface variability, *Continental Shelf Research*, 6(1-2), 31–51, [https://doi.org/10.1016/0278-4343\(86\)90052-x](https://doi.org/10.1016/0278-4343(86)90052-x).

- Dai, A., and K. E. Trenberth (2002), Estimates of Freshwater Discharge from Continents: Latitudinal and Seasonal Variations, *Journal of Hydrometeorology*, 3(6), 660–687, [https://doi.org/10.1175/1525-7541\(2002\)003<0660:eofdfc>2.0.co;2](https://doi.org/10.1175/1525-7541(2002)003<0660:eofdfc>2.0.co;2).
- Del Vecchio, R. (2004), Influence of the Amazon River on the surface optical properties of the western tropical North Atlantic Ocean, *Journal of Geophysical Research*, 109(C11), <https://doi.org/10.1029/2004jc002503>.
- Donlon, C., B. Berruti, A. Buongiorno, M.-H. Ferreira, P. Féménias, J. Frerick, P. Goryl, U. Klein, H. Laur, C. Mavrocordatos, J. Nieke, H. Rebhan, B. Seitz, J. Stroede, and R. Sciarra (2012), The Global Monitoring for Environment and Security (GMES) Sentinel-3 mission, *Remote Sensing of Environment*, 120, 37–57, <https://doi.org/10.1016/j.rse.2011.07.024>.
- Ecuador & Galapagos Insiders (2023), Amazon Rainforest Monthly Weather and Temperatures, <https://galapagosinsiders.com/travel-blog/climate-weather-amazon-rainforest-temperatures/>.
- Fore, A., S. Yueh, W. Tang, and A. Hayashi (2016), *SMAP Salinity and Wind Speed Data User's Guide, Version 3.0*, California Institute of Technology.
- Geyer, W. R., R. C. Beardsley, S. J. Lentz, J. Candela, R. Limeburner, W. E. Johns, B. M. Castro, and I. D. Soares (1996), Physical oceanography of the Amazon shelf, *Continental Shelf Research*, 16(5-6), 575–616, [https://doi.org/10.1016/0278-4343\(95\)00051-8](https://doi.org/10.1016/0278-4343(95)00051-8).
- Giffard, P., W. Llovel, J. Jouanno, G. Morvan, and B. Decharme (2019), Contribution of the Amazon River Discharge to Regional Sea Level in the Tropical Atlantic Ocean, *Water*, 11(11), 2348, <https://doi.org/10.3390/w11112348>.
- Hu, C., E. Montgomery, R. Schmitt, and F. Mullerkarger (2004), The dispersal of the Amazon and Orinoco River water in the tropical Atlantic and Caribbean Sea: Observation from space and S-PALACE floats, *Deep Sea Research Part II: Topical Studies in Oceanography*, 51(10-11), 1151–1171, [https://doi.org/10.1016/s0967-0645\(04\)00105-5](https://doi.org/10.1016/s0967-0645(04)00105-5).
- Jeffrey, S. W., and G. F. Humphrey (1975), New spectrophotometric equations for determining chlorophylls a, b, c1 and c2 in higher plants, algae and natural phytoplankton, *Biochimie und Physiologie der Pflanzen*, 167(2), 191–194, [https://doi.org/10.1016/s0015-3796\(17\)30778-3](https://doi.org/10.1016/s0015-3796(17)30778-3).
- Jo, Y.-H. (2005), A study of the freshwater discharge from the Amazon River into the tropical Atlantic using multi-sensor data, *Geophysical Research Letters*, 32(2), <https://doi.org/10.1029/2004gl021840>.
- Kurihara, Y. (2020), GCOM-C/SGLI Sea Surface Temperature (SST) ATBD (V.2), https://suzaku.eorc.jaxa.jp/GCOM_C/data/ATBD/ver2/V2ATBD_O1AB_SST_Kurihara_r1.pdf.
- Le, C., J. C. Lehrter, C. Hu, H. MacIntyre, and M. W. Beck (2017), Satellite observation of particulate organic carbon dynamics on the Louisiana continental shelf, *Journal of Geophysical Research: Oceans*, 122(1), 555–569, <https://doi.org/10.1002/2016jc012275>.
- Le, C., X. Zhou, C. Hu, Z. Lee, L. Li, and D. Stramski (2018), A Color-Index-Based Empirical Algorithm for Determining Particulate Organic Carbon Concentration in the Ocean From Satellite Observations, *Journal of Geophysical Research: Oceans*, 123(10), 7407–7419, <https://doi.org/10.1029/2018JC014014>.
- Lellouche, J.-M., E. Greiner, R. Bourdallé-Badie, G. Garric, A. Melet, M. Drévillon, C. Bricaud, M. Hamon, O. L. Galloudec, C. Regnier, T. Candela, C.-E. Testut, F. Gasparin, G. Ruggiero, M. Benkiran, Y. Drillet, and P.-Y. L. Traon (2021), The Copernicus Global 1/12° Oceanic and Sea Ice GLORYS12 Reanalysis, *Frontiers in Earth Science*, 9, <https://doi.org/10.3389/feart.2021.698876>.
- Lentz, S. J., and R. Limeburner (1995), The Amazon River Plume during AMASSEDs: Spatial characteristics and salinity variability, *Journal of Geophysical Research*, 100(C2), 2355, <https://doi.org/10.1029/94jc01411>.
- Liang, Y.-C., M.-H. Lo, C.-W. Lan, H. Seo, C. C. Ummenhofer, S. Yeager, R.-J. Wu, and J. D. Steffen (2020), Amplified seasonal cycle in hydroclimate over the Amazon river basin and its plume region, *Nature Communications*, 11(1), <https://doi.org/10.1038/s41467-020-18187-0>.
- Liu, D., D. Pan, Y. Bai, X. He, D. Wang, J.-A. Wei, and L. Zhang (2015), Remote Sensing Observation of Particulate Organic Carbon in the Pearl River Estuary, *Remote Sensing*, 7(7), 8683–8704, <https://doi.org/10.3390/rs70708683>.

- Lyakhin, Y. I. (1990), *Hydrochemistry of tropical regions of the World Ocean*, 213 pp., Gidrometeoizdat, Leningrad (in Russian).
- Magliocca, A. (1971), Some chemical aspects of the marine environment off the Amazon and Pará rivers, Brazil, *Boletim do Instituto Oceanográfico*, 20(1), 61–84, <https://doi.org/10.1590/S0373-55241971000100005>.
- Monin, A. S., and V. V. Gordeev (1988), *Amazonia*, 217 pp., Nauka, Moscow (in Russian).
- Muller-Karger, F. E., C. R. McClain, and P. L. Richardson (1988), The dispersal of the Amazon's water, *Nature*, 333(6168), 56–59, <https://doi.org/10.1038/333056a0>.
- Murakami, H. (2020), ATBD of GCOM-C chlorophyll-a concentration algorithm, https://suzaku.eorc.jaxa.jp/GCOM_C/data/ATBD/ver2/V2ATBD_O3AB_Chla_Murakami.pdf.
- NASA Ocean Biology Processing Group (2018), MODIS-TERRA Level 3 Mapped Particulate Organic Carbon Data Version R2018.0, <https://doi.org/10.5067/TERRA/MODIS/L3M/POC/2018>.
- NASA Ocean Biology Processing Group (2020a), MODIS Aqua Global Level 3 Mapped SST. Ver. 2019.0. PO.DAAC, <https://oceancolor.gsfc.nasa.gov/l3/>, (dataset accessed: 2022-11-24).
- NASA Ocean Biology Processing Group (2020b), MODIS Terra Global Level 3 Mapped SST. Ver. 2019.0. PO.DAAC, <https://oceancolor.gsfc.nasa.gov/l3/>, (dataset accessed: 2022-11-24).
- NASA Ocean Biology Processing Group (2021), SeaHawk HawkEye Level 1A Data, <https://doi.org/10.5067/SEAHAWK/HAWKEYE/L1/1>.
- NASA Ocean Biology Processing Group (2022), Aqua MODIS Level 3 Mapped Particulate Organic Carbon Data, Version R2022.0, <https://doi.org/10.5067/AQUA/MODIS/L3M/POC/2022>.
- Nordin, C. F., and R. H. Meade (1985), The Amazon and the Orinoco, in *Yearbook of science and technology*, pp. 385–390, McGraw-Hill Education.
- Reynolds, R. W., V. F. Banzon, and NOAA CDR Program (2008), NOAA Optimum Interpolation 1/4 Degree Daily Sea Surface Temperature (OISST) Analysis, Version 2, <https://doi.org/10.7289/V5SQ8XB5>.
- Smith, W. O., and D. J. Demaster (1996), Phytoplankton biomass and productivity in the Amazon River plume: correlation with seasonal river discharge, *Continental Shelf Research*, 16(3), 291–319, [https://doi.org/10.1016/0278-4343\(95\)00007-N](https://doi.org/10.1016/0278-4343(95)00007-N).
- Son, S., and M. Wang (2012), Water properties in Chesapeake Bay from MODIS-Aqua measurements, *Remote Sensing of Environment*, 123, 163–174, <https://doi.org/10.1016/j.rse.2012.03.009>.
- Stramski, D., R. A. Reynolds, M. Babin, S. Kaczmarek, M. R. Lewis, R. Röttgers, A. Sciandra, M. Stramska, M. S. Twardowski, B. A. Franz, and H. Claustre (2008), Relationships between the surface concentration of particulate organic carbon and optical properties in the eastern South Pacific and eastern Atlantic Oceans, *Biogeosciences*, 5(1), 171–201, <https://doi.org/10.5194/bg-5-171-2008>.
- Varona, H. L., D. Veleza, M. Silva, M. Cintra, and M. Araujo (2019), Amazon River plume influence on Western Tropical Atlantic dynamic variability, *Dynamics of Atmospheres and Oceans*, 85, 1–15, <https://doi.org/10.1016/j.dynatmoce.2018.10.002>.
- Visbeck, M. (2002), Deep Velocity Profiling Using Lowered Acoustic Doppler Current Profilers: Bottom Track and Inverse Solutions, *Journal of Atmospheric and Oceanic Technology*, 19(5), 794–807, [https://doi.org/10.1175/1520-0426\(2002\)019<0794:dvpula>2.0.co;2](https://doi.org/10.1175/1520-0426(2002)019<0794:dvpula>2.0.co;2).
- Wang, M., X. Liu, L. Jiang, and S. Son (2017), *The VIIRS Ocean Color Products, Algorithm Theoretical Basis Document, Version 1.0*, NOAA STAR.
- Yu, D., S. Liu, G. Li, Y. Zhong, J. Liang, J. Shi, X. Liu, and X. Wang (2022), The River-Sea Interaction off the Amazon Estuary, *Remote Sensing*, 14(4), 1022, <https://doi.org/10.3390/rs14041022>.